

CLEAVAGE FRACTURE IN MIXED MICROSTRUCTURES

Y. Hagiwara\* and J.F. Knott\*\*

\* Products Research and Development Labs., Nippon Steel Corporation, Sagamihara, Kanagawa, Japan.

\*\* Dept. of Metallurgy and Materials Science, University of Cambridge, England, U.K.

ABSTRACT

Fracture toughness values have been measured for martensitic and mixed martensitic-bainitic microstructures in HY80 steel. Increasing amounts of upper-bainite in the martensite matrix clearly lower the resistance to cleavage fracture. For the mixed microstructures, there is a rather wide scatter in fracture toughness values, and a model for estimating the fracture toughness of mixed microstructures is proposed. This is derived by assuming that the toughness of mixed microstructures possesses a bimodal Gaussian distribution. Predictions made from this model are seen to be in good agreement with the experimental results. The controlling factors for cleavage fracture in mixed microstructures are deduced, from fractographic examination, to be the amount of upper-bainite and its location with respect to the region of high stress ahead of a crack tip.

KEYWORDS

Transgranular cleavage fracture, mixed microstructure, bimodal toughness distribution, cleavage facets, critical distance, critical tensile stress, "cleavage fracture sensitivity factor".

INTRODUCTION

Mixed microstructures (low-carbon martensite and upper-bainite) can often occur in the heat-affected-zones (H.A.Z.s) of low-alloy structural steels, such as HY80 or A533B, and seem to represent the worst possible condition with respect to cleavage fracture. Dolby and Knott (1972) have demonstrated, by fracture toughness tests on martensite and upper-bainite H.A.Z.-simulated microstructures, that the introduction of upper-bainite into martensite of constant prior-austenite grain size progressively lowers the toughness when initiation is produced by quasi-cleavage. It appears, however, that few investigations have been carried out, making fracture toughness measurements on mixed microstructures having various controlled percentages of upper-bainite in martensite, and that little work has been carried out on the micro-mechanisms of cleavage fracture in such microstructures.

The most commonly accepted criterion for cleavage fracture is described in terms



of a critical tensile stress (Knott, 1977). Cleavage fracture occurs when the local tensile stress ahead of the notch tip exceeds a critical value. For sharply-notched specimens, a critical tensile stress has been successfully correlated with the plane-strain fracture toughness ( $K_{IC}$ ) in mild steel, by Ritchie, Knott and Rice (1973), assuming that such tensile stress should be exceeded over some microstructurally determined 'critical distance' ahead of the tip of the pre-crack (RKR model). Although this model was originally applied to normalized mild steel, some recent results on A533B steel, by Parks (1976), Green (1975) and Ritchie, Server and Wullaert (1979), have shown that this RKR model is very promising in its ability to predict  $K_{IC}$  on low-carbon bainitic steel.

More recently, Curry and Knott (1976, 1978, 1979) have demonstrated, using low- and medium-carbon steels, heat-treated to produce various size of plate-like and spheroidal carbides, that the 'critical distance' is determined by the statistical competition between numerous smaller carbide particles and less numerous larger particles. Low toughness is associated with a high probability of many large carbides being situated in the critical high-stress region ahead of the tip of the crack.

The aim of the present study was to determine the micromechanisms and factors controlling the cleavage fracture of mixed microstructures, by examining the variation of fracture toughness with the volume fraction of bainite in martensite.

#### EXPERIMENTAL PROCEDURE

The steel used was a low-alloy Ni-Cr-Mo steel (HY80), whose chemical composition is shown in Table 1. Specimens were austenitised at 1200°C for 2 hours and were then either oil quenched, to produce 100% martensite, or isothermally-transformed at 480°C for various hold times to give varying amounts of upper-bainite in the martensite matrix. Fracture toughness specimens were machined in the single-edge-notched (SEN) bend geometry, (TL orientation), having a length of 100mm, thickness,  $B = 23\text{mm}$  and width,  $W = 20\text{mm}$ . These were pre-cracked in fatigue under conditions as specified in BS5447, and fracture toughness tests were performed in three-point bend over a range of temperatures from -196°C to -60°C, using a 100kN MAND servo-hydraulic machine. Also, values of critical tensile fracture stress ( $\sigma_F$ ) were determined by testing, in four-point bend, specimens having the geometry corresponding to that analysed by Griffiths and Owen (1971). The uniaxial tensile properties were obtained using Hounsfield No.13 specimens. Each fractured specimen was nickel-plated and sectioned at mid-thickness. The percentage of upper-bainite was measured using a systematic point-counting technique around the tip of the fatigue pre-crack. Fracture surfaces were examined in the scanning electron microscope (SEM).

TABLE 1. Chemical composition of HY80

C	Mn	Si	P	S	Ni	Cr	Mo
0.18	0.35	0.23	0.012	0.012	2.89	1.67	0.51

#### RESULTS

Optical micrographs of typical martensite and martensite-bainite microstructures are shown in Fig. 1.

Figure 2 shows the variation of critical COD ( $\delta_c$ ) with test temperature, and Fig. 3 shows the fracture toughness ( $K_{IC}$ ) as a function of the proportion of upper-bainite ( $\beta$ ) at a temperature of -142±3°C. These were all 'valid'  $K_{IC}$  results.

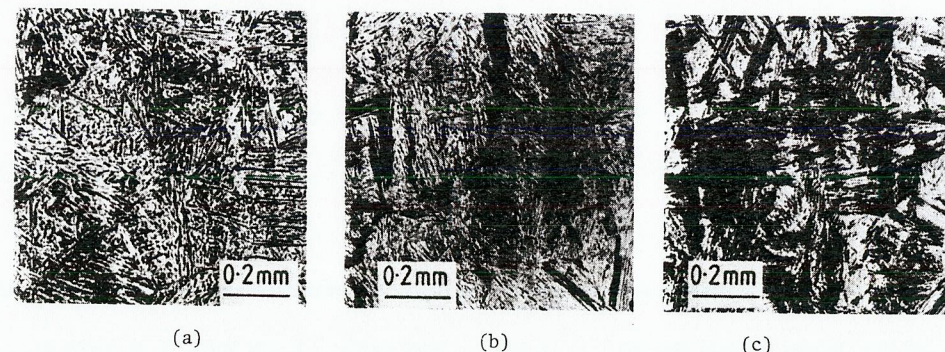


Fig. 1. Typical microstructures: (a) 100% martensite, (b) 22% bainite, (c) 70% bainite. The darker-etching constituent is bainite.

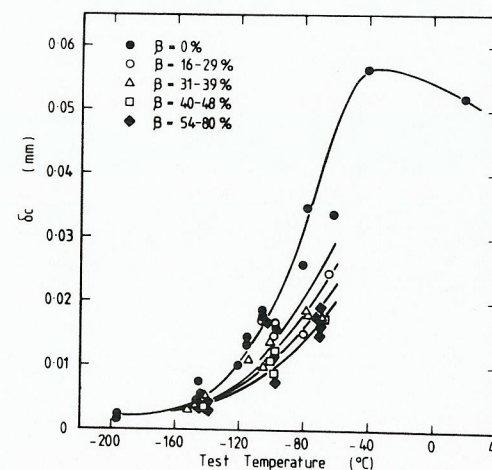


Fig. 2. Variation of critical COD ( $\delta_c$ ) with test temperature.

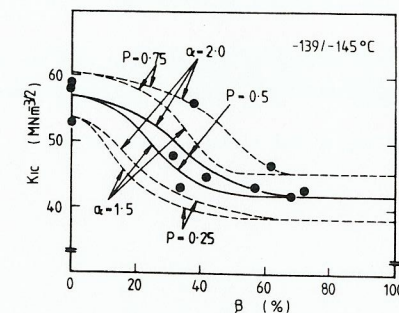


Fig. 3. Variation of fracture toughness ( $K_{IC}$ ) with bainite percentage ( $\beta$ ) in the mixed microstructures, tested at -142±3°C. (Estimation:  $K_{IC}^0 = 57\text{MNm}^{-3/2}$ ,  $K_{IC}^{100} = 42\text{MNm}^{-3/2}$ , standard deviation =  $5\text{MNm}^{-3/2}$ ).

Fractographic examination of the fracture surfaces, in the SEM, revealed that all fractures tested below -139°C were completely quasi-cleavage, as seen in Fig. 4(a,b). The cleavage facets (Fig. 4b) associated with bainite were larger, compared with those associated with martensite (Fig. 4a). The fractures above -139°C showed a 'mixed-mode' of cleavage and microvoid coalescence, e.g. Fig. 4(c). Fig. 5 shows an optical micrograph of a nickel-plated fracture edge. It is clear that the quasi-cleavage fracture in the mixed microstructures is associated with bainite, and that microvoid coalescence is associated with martensite.



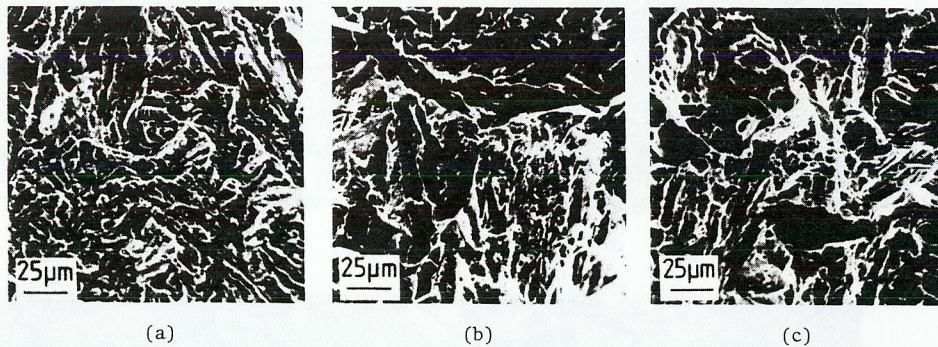


Fig.4. Fracture surfaces: (a) 100% martensite tested at -145°C, (b) 72% bainite tested at -144°C, (c) 35% bainite tested at -68°C.

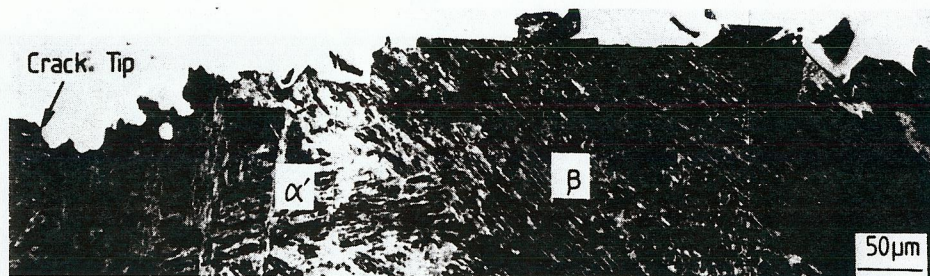


Fig.5. Nickel-plated fracture profile of 35% bainite tested at -68°C (bainitic regions are marked  $\beta$ ; martensitic regions  $\alpha'$ ).

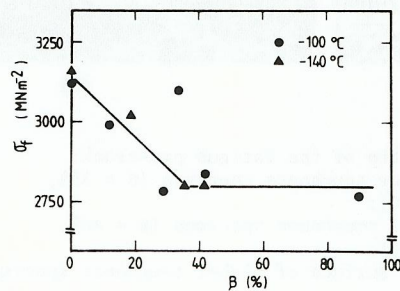


Fig.6. Variation of critical tensile stress ( $\sigma_f$ ) with bainite percentage ( $\beta$ ) in the mixed microstructures tested at -100°C and -140°C.

It can be seen from Figs. 2 and 3 that for small amounts of bainite, the fracture toughness decreases rapidly with increase of  $\beta$ , and that at higher proportions ( $\beta > 50\%$ ), it remains almost constant. There is a rather larger scatter in the toughness values for mixed microstructures than for single microstructures. The reason for this scatter will be discussed in the following section. Apparently similar results were obtained at test temperatures of about -100°C and -70°C, but are more difficult to interpret because the fracture mode is mixed.

Figure 6 shows the variation of the critical tensile fracture stress,  $\sigma_f$  (measured in V-notched bars) with the percentage of bainite ( $\beta$ ). These tests were carried out at temperatures in the range -143°C to -100°C. Almost constant values of  $\sigma_f$  were obtained over this temperature range if specimens had the same microstructures, and compare reasonably with earlier results for similar bainitic microstructures (Knott, 1977). Again,  $\sigma_f$  decreases rapidly when a small proportion of bainite is introduced in martensite structure and appears to remain constant for  $\beta > 40\%$ .

#### DISCUSSION

From Fig.3, a simple model might be that  $K_{IC}$  values for mixed microstructures lie between two limits, corresponding to 100% martensite and 100% bainite, and we have examined the literature to try to find other examples of "bimodal" toughness. Newmann, Benois and Hilbert (1968) demonstrated the existence of a bimodal distribution in Charpy V-notch energy values for low-hydrogen weld metal in the transition temperature region. Each toughness individually seemed to fit a Gaussian distribution. Similarly, Wilshaw and Pratt (1965) observed bimodal behaviour in the cleavage toughness of mild steel. We proceed to examine the consequences of a bimodal distribution.

To simplify the analysis of the scatter, a Gaussian distribution of fracture toughness ( $K_{IC}$ ) in both martensite ( $K_{IC}^0 = K_{IC}$  at  $\beta = 0\%$ ) and upper-bainite ( $K_{IC}^{100} = K_{IC}$  at  $\beta = 100\%$ ) is assumed with the same standard deviation ( $S$ ) in each case. The probability ( $P(K_{IC})$ ) of  $K = K_{IC}$  in a mixed microstructure having a proportion of bainite  $\beta$ , may be written as:

$$P(K_{IC}) = [(1-\alpha\beta) \int_{-\infty}^X + \alpha\beta \int_{-\infty}^Y] \exp(-u^2/2) / \sqrt{2\pi} du \quad (1)$$

$$X = (K_{IC} - K_{IC}^0) / S$$

$$Y = (K_{IC} - K_{IC}^{100}) / S$$

where  $\alpha$  is defined as the cleavage fracture sensitivity factor of bainite compared with martensite.

Using the appropriate values of fracture toughness,  $K_{IC}^0$  and  $K_{IC}^{100}$ , and a standard deviation,  $S$  at a given temperature, the most probable average ( $P(K_{IC}) = 0.5$ ) relationship between  $K_{IC}$  and  $\beta$  can be calculated as a function of  $\alpha$ . The estimated variations of  $K_{IC}$  with  $\beta$  are shown in Fig.3 with solid lines, where  $K_{IC}^0 = 57 \text{ MNm}^{-3/2}$ ,  $K_{IC}^{100} = 42 \text{ MNm}^{-3/2}$  and  $S = 5 \text{ MNm}^{-3/2}$  are assumed. (A scatter of  $\pm 10\%$  on  $K_{IC}$  is not unreasonable). Taking these values, agreement between estimated and experimental results is obtained, if the fracture sensitivity factor is taken as  $\alpha = 1.5 \sim 2.0$ . The choice of  $\alpha$  is, at this stage, arbitrary, but finds justification in the micro-mechanics of the fracture process, as follows.

From examination of the SEM micrographs of cleavage fracture surfaces, the mean diameter of the cleavage facets ( $L_c$ ) was determined by means of the linear intercept technique:  $L_c^0 = 10 \mu\text{m}$  for martensite and  $L_c^{100} = 38 \mu\text{m}$  for bainite. Work on



cleavage fracture of low-carbon martensites and bainites (Dolby and Knott, 1972; Naylor, 1976; Brozzo and others, 1977) has established that the predominant microstructural parameter of cleavage fracture in lath microstructures is the packet size. If  $L_c$  is the crack nucleus size, i.e. that of the most favourably orientated packet, and can propagate into adjoining packets only if extra work is done, the ratio,  $\alpha = (L_c^{100}/L_c^0)^{1/2}$  is seen to represent the cleavage fracture sensitivity factor of bainite compared with martensite. This value is calculated to be 1.9, which agrees well with the values deduced from the comparison between prediction and experiment of the variation of  $K_{IC}$  with  $\beta$  ( $\alpha = 1.5 \sim 2.0$ ).

Predictions of  $K_{IC}$  vs.  $\beta$  for  $P(K_{IC}) = 0.25$  and  $0.75$  are also shown in Fig.3 with dotted lines. About 50% of data will be expected to lie between these two curves. It is found that these estimations in fact give reasonable upper and lower bound to the fracture toughness values, but this is presumably because only a limited number of tests has been performed. The results support the postulate that the scatter in toughness for mixed microstructures is derived from the bimodal distribution of the fracture toughness. Both the trend in  $K_{IC}$  decreasing with increasing  $\beta$ , and the larger scatter of  $K_{IC}$  in mixed microstructures, can be estimated by assuming normal distributions for the individual toughnesses of martensite and bainite.

Figure 7 shows SEM micrographs of fracture surfaces of two widely-separated fracture toughness values for microstructures having almost the same bainite constituent (e.g. the two data points at  $\beta \approx 40$  in Fig.3). Both specimens fractured in a cleavage manner. Figs. 7(a) and (b) illustrate the general view of fracture surfaces along the tip of the crack around the mid-thickness position of the specimen. Ritchie, Knott and Rice (1973) have shown that the critical distance,  $X_0$  can be calculated, using FEM stress analysis for a sharp notch, from the parameters; fracture toughness, cleavage fracture stress and yield stress. In the present study, the critical distances were  $62\mu\text{m}$  and  $46\mu\text{m}$  for martensite and 80% bainite microstructures, respectively, using Tracey's results (1976). The critical distances are shown on the fracture surfaces in Figs. 7(a) and 7(b). It can be seen that large cleavage facets associated with upper-bainite lie almost entirely along the crack tip for the lower toughness specimen, as shown in Fig.7(d). On the other hand, smaller cleavage facets, associated with martensite (e.g. Fig.7(c), compared with Fig.4(a) observed on a 100% martensite fracture surface), were found ahead of the tip of the fatigue crack, for the higher toughness specimen, especially in the region within critical distance. It may therefore be concluded that the fracture toughness of mixed microstructures is affected not only by the proportion of bainite per se but also by its location ahead of the crack tip, that is, by the probability of coarse bainite occurring in regions where the stress is high. This also gives the basic reason for the statistical nature of cleavage fracture in mixed microstructures, which is attributed to the chance of high-stress regions being coincident with 'tough' or 'brittle' microstructural components. This argument is similar to that of Curry and Knott (1979) except that the 'brittle' phases are now bainite packets rather than carbide particles.

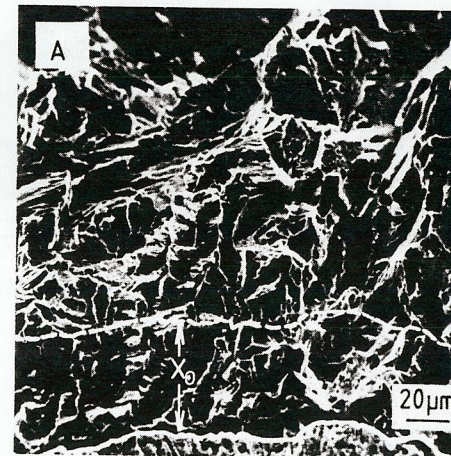
A further important 'mixed microstructure' is found in C/Mn weld metals, where the ferrite is distributed in coarse 'pro-eutectoid' and fine 'acicular' forms (Widgery, 1976). Presumably, the pro-eutectoid form would behave in a manner similar to that of the bainite in the present experiments and the acicular form could be compared with the martensite. A probability analysis similar to that in equation (1) might then be able to explain the 'bimodal' behaviour observed by Newmann, Benois and Hilbert (1968). The results of Wilshaw and Pratt (1965) in wrought material are more difficult to explain. Their description of the microstructure specified 'uniform' grain size ( $40\mu\text{m}$ ) but mentioned cementite in 'massive coalesced form' at grain boundaries and also 'enveloping small islands of coarse pearlite'. These carbides will be relatively 'brittle' phases and the



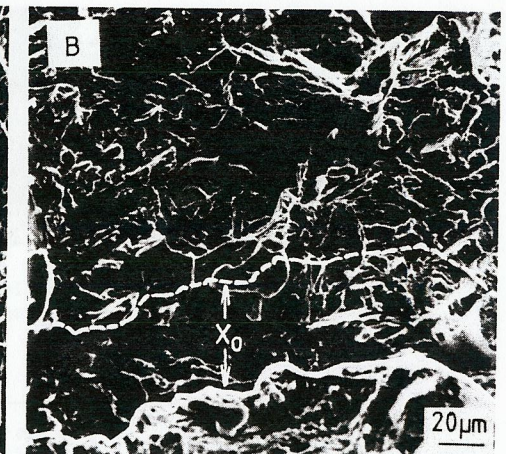
(a)



(b)



(c)



(d)

Fig.7. Fracture surfaces at the tip of the fatigue pre-crack:  
 (a) General view of higher toughness specimen ( $\beta = 38\%$ ,  $K_{IC} = 56.0 \text{ MNm}^{-3/2}$ ,  $-142^\circ\text{C}$ );  
 (b) General view of lower toughness specimen ( $\beta = 42\%$ ,  $K_{IC} = 44.7 \text{ MNm}^{-3/2}$ ,  $-142^\circ\text{C}$ );  
 (c) Martensitic fracture surface of higher toughness specimen (high magnification of A);  
 (d) Bainitic fracture surface of lower toughness specimen (high magnification of B).



bimodal behaviour could arise from the presence or absence of such carbides in the high stress region ahead of a Charpy V-notch. Since the stress gradients ahead of V-notches are less severe than those ahead of cracks, it might be necessary also to invoke some 'banding' of microstructure to explain the bimodal behaviour.

#### ACKNOWLEDGEMENTS

The authors wish to thank Professor R.W.K. Honeycombe for provision of laboratory facilities. Financial support from Nippon Steel Corporation of Japan is gratefully acknowledged by one of the authors (YH) during the course of this study at Cambridge.

#### REFERENCES

- Brozzo, P., Buzzichelli, G., Mascanzoni, A. and Mirabile, M. (1977). Metal Science, 11, 123-129.
- Curry, D.A. and Knott, J.F. (1976). Metal Science, 10, 1-6.
- Curry, D.A. and Knott, J.F. (1978). Metal Science, 12, 511-514.
- Curry, D.A. and Knott, J.F. (1979). Metal Science, 13, 341-345.
- Dolby, R.E. and Knott, J.F. (1972). J. Iron and Steel Inst., 210, 857-865.
- Green, G. (1975) Ph.D. Thesis, Cambridge University.
- Griffiths, J.R. and Owen, D.R. (1971). J. Mech. Phys. Solids, 19, 419-431.
- Knott, J.F. (1977). In D.M.R. Taplin (Ed.), Fracture 1977, Vol.1, University of Waterloo Press, 61-92.
- Naylor, J. (1976). Grain Boundaries, Jersey, Inst. of Metallurgists, F.13.
- Newmann, A., Benois, F.F. and Hilbert, K. (1968). Schweisstechnik (Berlin), 18, 385-390.
- Parks, D.M. (1976). J. Eng. Materials and Technology, 98, 30-36.
- Ritchie, R.O., Knott, J.F. and Rice, J.R. (1973). J. Mech. Phys. Solids, 21, 395-410.
- Ritchie, R.O., Server, W.L. and Wullaert, R.A. (1979). Proc. 3rd. ICM., Vol.3. Cambridge, 489-500.
- Tracey, D.M. (1976). J. Eng. Materials and Technology, 98, 146-151.
- Widgery, D.J. (1976). Welding Research Supplement, Mar., 57s-68s.
- Wilshaw, T.R. and Pratt, P.L. (1965). Proc. 1st. Int. Conf. on Fracture, Sendai, Japan, 973-991.